

# INTERFACE CRACK GROWTH BY VOID EXPANSION MECHANISMS BETWEEN DUCTILE SOLID AND ELASTIC SUBSTRATE

V. Tvergaard

Department of Mechanical Engineering, Solid Mechanics  
Technical University of Denmark, DK-2800 Kgs. Lyngby, Denmark

## ABSTRACT

Crack growth along an interface between an elastic-plastic solid and an elastic substrate is analysed numerically by using a special cohesive zone formulation, in which the modified Gurson model is applied to describe ductile failure. Small scale yielding conditions are applied with mixed mode loading prescribed on the outer edge of the region analysed.

## 1. INTRODUCTION

For interface crack growth by a ductile failure mechanism special cohesive zone elements are used to represent the fracture process zone. The modified Gurson model is used in the cohesive zone elements to represent the nucleation and growth of voids to coalescence, as has been done for symmetric mode I loading by Tvergaard [1]. In the present study for mixed mode loading on a bi-material interface a small scale yielding formulation is used, with the corresponding displacement fields prescribed on the outer boundary of the region analysed, as in [2,3].

In relation to the finite element mesh the initial width of the interface is taken to be zero, but the traction separation relations represented by the cohesive zone are based on assuming an interface width of the order of the void spacing. The present study for an interface between an elastic-plastic solid and an elastic substrate is a continuation of the studies by Tvergaard [4] for an interface between dissimilar elastic-plastic materials. A somewhat related cohesive zone formulation has been used by Siegmund and Brocks [5], where the level of the stress triaxiality to be used in the Gurson model is taken from the stress level in the material adjacent to the cohesive zone. The present cohesive zone model formulation does not make use of field quantities from the neighbouring finite elements, but instead continuity of the longitudinal strain along the band is required, across the band interfaces, and this compatibility requirement together with the loads carried across the interface determines the evolution of stresses and strains in the interface layer.

## 2. COHESIVE ZONE MODEL FOR DUCTILE FAILURE

The initial width of the special cohesive zone for ductile failure is taken to be zero, as in other cohesive zone calculations [2,6], but the traction-separation properties of the cohesive zone elements are calculated based on a background element with the non-zero initial width  $w_0$ . Fig. 1a illustrates the finite element mesh near the crack plane, with the background interface element sketched in, while Fig. 1b indicates the configuration if this interface element is attached to the surrounding elements as a common element. The displacement components on the top side of the element are denoted by  $u_n^+$  and  $u_t^+$ , respectively, while those on the bottom side of the element are denoted by  $u_n^-$  and  $u_t^-$  (see Fig. 1a). These displacements are required to be compatible with

the displacements on the edge of the adjacent finite elements. Then, with the assumptions that the displacements inside the interface element vary linearly through the element width (in the  $x^2$  - direction) and with the gradients replaced by their averages through the element width, the displacement gradients inside the elements are approximated as

$$\frac{\partial u_1}{\partial x^2} = \frac{u_t^+ - u_t^-}{w_0}, \quad \frac{\partial u_2}{\partial x^2} = \frac{u_n^+ - u_n^-}{w_0} \quad (1)$$

$$\frac{\partial u_1}{\partial x^1} = \frac{1}{2} \left( \frac{\partial u_t^+}{\partial x^1} + \frac{\partial u_t^-}{\partial x^1} \right), \quad \frac{\partial u_2}{\partial x^1} = \frac{1}{2} \left( \frac{\partial u_n^+}{\partial x^1} + \frac{\partial u_n^-}{\partial x^1} \right) \quad (2)$$

From the expressions (1) and (2) for the displacement gradients, and from their increments, it is possible to determine the current metric tensor  $G_{ij}$ , the Lagrangian strain tensor  $\eta_{ij}$  and its increment  $\dot{\eta}_{ij}$  in any point on the middle surface,  $x^2 = 0$ , of the interface element, and thus a set of constitutive relations can be used to calculate the evolution of stresses and the evolution of damage inside the interface. These constitutive relations are based on the modified Gurson model [7,8], which makes use of an approximate yield condition for the porous solid is of the form

$$\Phi = \frac{\sigma_e^2}{\sigma_M^2} + 2q_1 f^* \cosh \left[ \frac{\sigma_k^k}{2\sigma_M} \right] - 1 - (q_1 f^*)^2 = 0 \quad (3)$$

where  $\sigma_e = (3s_{ij}s^{ij}/2)^{1/2}$  and  $s^{ij} = \sigma^{ij} - G^{ij}\sigma_k^k/3$ . The void volume fraction is  $f$  and  $f^*(f)$  is a function that approximately describes final failure by void coalescence.

The numerical solutions are obtained by a linear incremental finite element model, based on the incremental principle of virtual work. As described in [1,4], an extra parameter  $r_0$  is introduced, to be able to reduce the tangential components of the nodal forces calculated by the interface element procedure described above. The tensile or compressive stress components  $\sigma_{11}$  along the interface layer are already fully accounted for in the finite element mesh outside the interface, due to the somewhat artificial overlap of the background interface element with the neighbouring element mesh

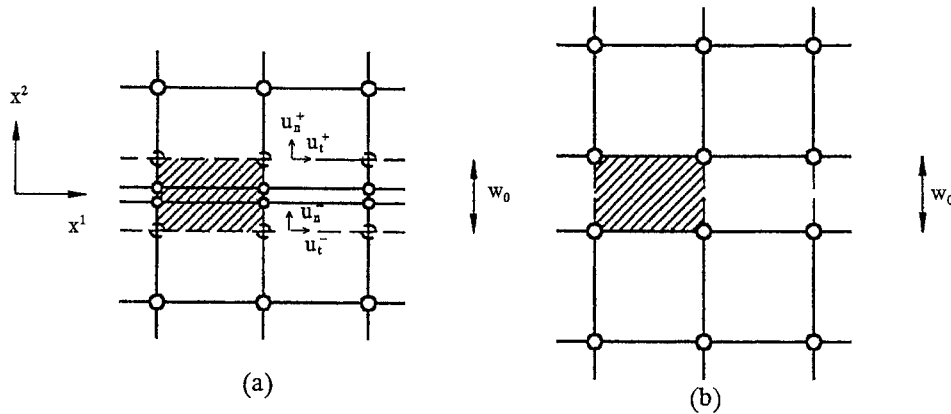


Fig. 1. Interface elements along the crack plane. (a) Shows the artificial overlap between interface elements and surrounding elements. (b) A corresponding configuration with no overlap.

(see Fig. 1a). On the other hand, the full size of the nodal forces normal to the interface is needed to carry the loads on the interface, and in the case of mixed mode loading the same is true for the part of the nodal forces tangential to the interface that results from shear loads on the interface.

The nodal forces on the top side of the interface element are denoted  $P_n^+$  and  $P_t^+$ , respectively, taken to be positive in the direction of  $u_n^+$  and  $u_t^+$ , and on the bottom side the force components  $P_n^-$  and  $P_t^-$  are positive in the directions of  $u_n^-$  and  $u_t^-$ . The nodal force components calculated by the standard element procedure are denoted by  $(P)_{\text{elm}}$ . For full mixed mode loading on the interface the reduction in the symmetric part of the tangential nodal forces obtained from the interface element is specified by taking the forces  $P_t^+$  and  $P_t^-$  to be given by [4]

$$P_t^+ = (P_t^+)_{\text{elm}} - \frac{1-r_0}{2} \left( (P_t^+)_{\text{elm}} + (P_t^-)_{\text{elm}} \right) \quad (4)$$

$$P_t^- = (P_t^-)_{\text{elm}} - \frac{1-r_0}{2} \left( (P_t^+)_{\text{elm}} + (P_t^-)_{\text{elm}} \right) \quad (5)$$

where  $r_0 = 0$  will be used, as this gives a representation of an initially sharp crack [1]. The value of the initial width  $w_0$  of the strip (Fig. 1) is non-zero, representing about 0.7 times the initial void spacing.

The crack is taken to grow along the interface between two materials, where material No. 1 is elastic-plastic, described by  $J_2$  flow theory, with the material parameters  $E_1$ ,  $\nu_1$ ,  $\sigma_{Y1}$  and  $N_1$ , while the substrate, material No. 2, is elastic with  $E_2$  and  $\nu_2$ . In all analyses here, the values of the material parameters inside the interface elements are taken to be identical to the values in material No. 1, thus representing a situation where failure occurs in the softer elastic-plastic material. Conditions of small scale yielding are used. The elastic singular fields, with amplitudes in the form of two stress intensity factor components  $K_I$  and  $K_{II}$  [2,3], have an oscillating singularity at the crack-tip. On the outer edge of the region analysed the displacement components corresponding to these fields are prescribed. For the presentation of results, a reference value of the  $J$ -integral is defined as  $J_0 = \sigma_{Y1} w_0$ , and the corresponding reference stress intensity factor (with the second Dunders' parameter  $\beta$ ) is defined as

$$K_0 = \left[ \frac{1-\nu_1^2}{E_1} + \frac{1-\nu_2^2}{E_2} \right]^{-1/2} \left( \frac{2J_0}{1-\beta^2} \right)^{1/2} \quad (6)$$

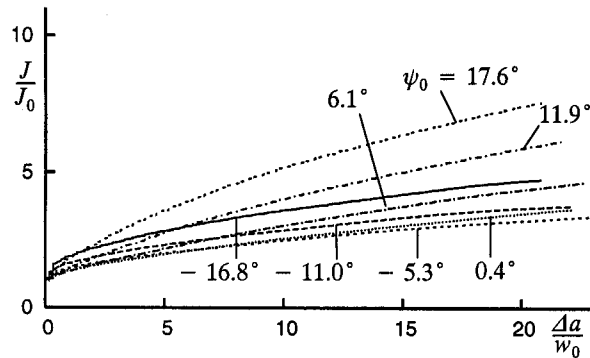


Fig. 2. Interface crack growth resistance curves for  $f_I = 0.01$  and  $f_N = 0$ .

A length quantity  $R_0$ , which scales with the size of the plastic zone in material No. 1 is defined in terms of  $K_0$  or  $J_0$  as

$$R_0 = \frac{1}{3\pi} \left( \frac{K_0}{\sigma_{Y1}} \right)^2 = \frac{2}{3\pi} \left[ \frac{1-\nu_1^2}{E_1} + \frac{1-\nu_2^2}{E_2} \right]^{-1} \frac{J_0}{(1-\beta^2)\sigma_{Y1}^2} \quad (7)$$

### 3. RESULTS

The properties of material No. 1 are specified by  $\sigma_{Y1}/E_1 = 0.002$ ,  $\nu_1 = 0.3$  and  $N_1 = 0.1$ , and these values of the material parameters are also used in the interface elements. The elastic substrate has  $\nu_2 = 0.3$  and is chosen to focus on a situation where the substrate has much higher elastic stiffness than that of material No. 1, such that  $E_2/E_1 = 1000$ . In the first set of calculations the porous ductile material inside the interface elements is taken to have voids present from the beginning, with the initial void volume fraction  $f_I = 0.01$  and no void nucleation, and the additional parameter value in (3) is chosen as  $q_1 = 1.25$ . The amount of crack growth  $\Delta a$  will here be normalised by the width  $w_0$  of the interface elements. It is noted that the reference length defined in (7) has the value  $R_0 = 126.8w_0$ , and that the mesh refinement in the computations is chosen so that  $\Delta_0 = w_0/2$ .

Computed crack growth resistance curves are shown in Fig. 2 for these values of the material parameters. The different resistance curves correspond to external loading with different mode mixity, as measured by the angle  $\psi_0$  that is defined in detail in [2,3,4]. It is noted that for  $\psi_0 = 0^\circ$  the conditions near the crack-tip are close to pure mode I loading ( $K_I$  dominates), while for  $\psi_0 \neq 0^\circ$  there is a significant contribution from  $K_{II}$  in addition to  $K_I$  (negative when  $\psi_0$  is negative and vice versa). It is seen in Fig. 2 that the lowest resistance curves are found for  $\psi_0 = 0.4^\circ$  or  $\psi_0 = -5.3^\circ$ , i.e. close to  $0^\circ$ . For larger negative or positive values of  $\psi_0$  the crack growth resistance is higher. But it is noted that since there is no material symmetry about the crack plane, the resistance for a negative value of  $\psi_0$  differs from that for the same positive value of  $\psi_0$ .

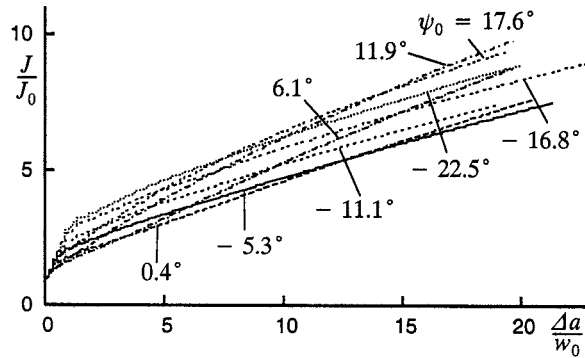


Fig. 3. Interface crack growth resistance curves for  $f_I = 0$ ,  $f_N = 0.04$ ,  $\varepsilon_N = 0.1$  and  $s_N = 0.1$ .

In the case of Fig. 3 there are no voids initially in the cohesive elements along the interface,  $f_I = 0$ , but plastic strain controlled nucleation of new voids takes place, as specified by a normal distribution with the volume fraction  $f_N = 0.04$  of void nucleating particles, the mean strain for nucleation  $\varepsilon_N = 0.1$  and the standard deviation  $s_N = 0.1$ . Here, the crack growth resistance keeps growing in the whole range analysed, and the resistances reached are significantly higher than those in Fig. 2. Again the lowest resistance curves correspond to the values  $0.4^\circ$  or  $-5.3^\circ$  of the angle  $\psi_0$ , in most of the range considered. Also, for higher or lower values of  $\psi_0$  the crack growth resistance increases.

The values of the material parameters in Fig. 4 are identical to those in Fig. 3, apart from the smaller volume fraction of void nucleating particles,  $f_N = 0.02$ , and the larger value of the mean strain for nucleation,  $\varepsilon_N = 0.2$ , inside the cohesive elements. This difference has a large effect as is seen by the much higher crack growth resistances predicted in Fig. 4.

The results in Figs. 2, 3 and 4 can be compared with results in [4] for the same set of material parameters in material No. 1 and in the cohesive zone, but for an elastic-plastic substrate specified by  $E_2/E_1 = 2$  and  $\sigma_{Y2}/\sigma_{Y1} = 2$ . It is found that the much higher elastic stiffness and the lack of plastic deformations in the substrate gives significantly higher resistance to interface crack growth.

The dependence of the crack growth resistance on mode mixity is illustrated in Fig. 5 by the values of the fracture toughness after a specific amount of crack growth,  $\Delta a/w_0 = 10$ , vs. the angle  $\psi_0$ . As in the cases considered in [4] it is seen that the minima of the three curves occur near the axis  $\psi_0 = 0^\circ$ , while larger toughness is found in the range of both negative and positive values of  $\psi_0$ .

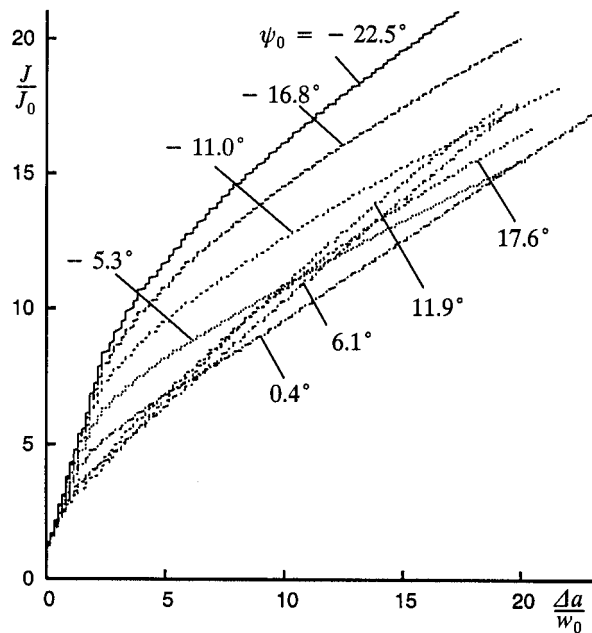


Fig. 4. Interface crack growth resistance curves for  $f_I = 0$ ,  $f_N = 0.02$ ,  $\varepsilon_N = 0.2$  and  $s_N = 0.1$ .

## REFERENCES

- [1] Tvergaard, V. Crack growth predictions by cohesive zone model for ductile fracture. *J. Mech. Phys. Solids* 49, 2191-2207, 2001.
- [2] Tvergaard, V. and Hutchinson, J.W. The influence of plasticity on mixed mode interface toughness. *J. Mech. Phys. Solids* 41, 1119-1135, 1993.
- [3] Tvergaard, V. Resistance curves for mixed mode interface crack growth between dissimilar elastic-plastic solids. *J. Mech. Phys. Solids* 49, 2689-2703, 2001.
- [4] Tvergaard, V. Predictions of mixed mode interface crack growth using a cohesive zone model for ductile fracture. *J. Mech. Phys. Solids* (in press).
- [5] Siegmund, T. and Brocks, W. Local fracture criteria: Lengthscales and applications. *J. Phys.* IV 8, 349-356, 1998.
- [6] Tvergaard, V. and Hutchinson, J.W. The relation between crack growth resistance and fracture process parameters in elastic-plastic solids. *J. Mech. Phys. Solids* 40, 1377- 1397, 1992.
- [7] Gurson, A.L. Continuum theory of ductile rupture by void nucleation and growth - I. Yield criteria and flow rules for porous ductile media. *J. Engrg. Materials Technol.* 99, 2-15, 1977.
- [8] Tvergaard, V. Material failure by void growth to coalescence. *Adv. App. Mech.* 27, 83-151, 1990.

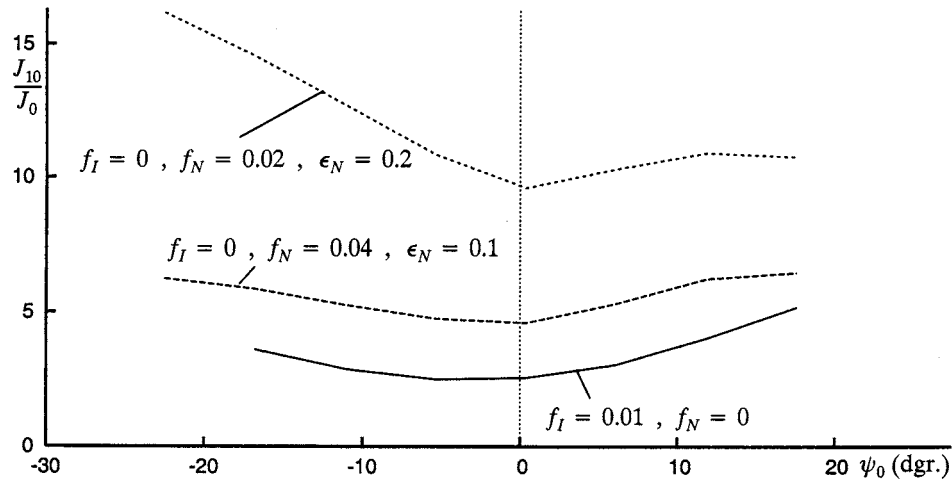


Fig. 5. Interface toughness  $J_{10}$ , at the point of the resistance curves where  $\Delta a/w_0 = 10$ , shown to indicate the dependence of toughness on the mode mixity parameter  $\psi_0$ .